

See discussions, stats, and author profiles for this publication at: <https://www.researchgate.net/publication/38076629>

Free Radical Scavenging Properties of Guaiacol Oligomers: A Combined Experimental and Quantum Study of the Guaiacyl-Moiety Role

ARTICLE in THE JOURNAL OF PHYSICAL CHEMISTRY A · NOVEMBER 2009

Impact Factor: 2.69 · DOI: 10.1021/jp906285b · Source: PubMed

CITATIONS

31

READS

50

8 AUTHORS, INCLUDING:



El Hassane Anouar

27 PUBLICATIONS 218 CITATIONS

SEE PROFILE



Pavlína Kosinová

Palacký University of Olomouc

5 PUBLICATIONS 676 CITATIONS

SEE PROFILE



Florent Di Meo

University of Limoges

24 PUBLICATIONS 209 CITATIONS

SEE PROFILE



Yves Champavier

University of Limoges

35 PUBLICATIONS 582 CITATIONS

SEE PROFILE

Free Radical Scavenging Properties of Guaiacol Oligomers: A Combined Experimental and Quantum Study of the Guaiacyl-Moiety Role

E. Anouar,^{†,‡} C. A. Calliste,[†] P. Košinová,[†] F. Di Meo,[†] J. L. Duroux,[†] Y. Champavier,[§] K. Marakchi,[‡] and P. Trouillas^{*,†}

Université de Limoges, EA 4021, Faculté de Pharmacie, 2 rue du Docteur Marcland, 87025 Limoges, France, Université Mohammed V, Laboratoire de Chimie Théorique, Faculté des Sciences, B.P 1014 Rabat, Morocco, and Service commun de RMN, Université de Limoges, 2 rue du Docteur Marcland, 87025 Limoges, France

Received: July 3, 2009; Revised Manuscript Received: October 5, 2009

Natural polyphenols are known to exhibit a lot of different biological properties, including antioxidant activity. For some polyphenols these activities are attributed to the presence of a guaiacol moiety. In the present paper we focus on the role of this moiety. For this purpose nine different compounds were enzymatically synthesized from guaiacol. To elucidate the structure–activity relationship of these polyphenols, DFT-(PCM)B3P86/6-311+G(2d,3pd)//(PCM)B3P86/6-31+G(d,p) calculations supported the experimental DPPH free radical scavenging activities. The antioxidant activities were correlated to (i) O–H BDEs (bond dissociation enthalpies), (ii) BDE_D (BDE of a second H atom abstraction from the phenoxyl radicals), (iii) spin density, (iv) HOMO (highest occupied molecular orbital) distribution, (v) IPs (ionization potentials), (vi) ΔG and ΔG^\ddagger free energies of HAT (H atom transfer), and (vii) HAT rate constants. BDE_D appeared to be the most important descriptor to understand the free radical scavenging ability of these compounds.

Introduction

Polyphenols including phenolic acids, flavonoids, lignans, procyanidins, and tannins constitute an important group of natural compounds. The large chemical structure variety of these compounds allows a range of chemical properties and thus numerous different biological activities.¹ In particular they are antioxidants (i.e., free radical scavengers, membrane lipid peroxidation inhibitors, oxidative enzyme inhibitors, metal chelators, ...).^{2–4} Most of them are phytonutrients since they are found in food (e.g., fruit, vegetables, wines, teas, and olive and argan oils).⁵ It is now well-admitted that their antioxidant properties are largely attributed to the OH group capacity to donate a hydrogen atom. This property is crucial to explain the polyphenol capacity to scavenge ROS (reactive oxygen species), implicated in different diseases (e.g., cardiovascular diseases, cancers, ...).³

In addition to the experimental studies,^{2–4} theoretical investigations based on quantum chemical calculations have managed, over the past 10 years, to establish the structure–antioxidant activity relationship of different series of polyphenolic compounds.^{6–21} The use of DFT (density functional theory) has become very popular since it successfully describes the H atom abstraction capacity of OH phenolic groups. In conclusion to all those different studies, it appears that the catechol moiety present in quercetin,^{12,16} catechin,^{9,20} luteolin,^{11,18} *nor*-dehydrosilybin,¹⁹ etc., strongly participates in the free radical scavenging capacity of flavonoids and other derivatives. The 3-OH group existing in flavonols (e.g., quercetin, myricetin, morin, kampferol) also partly contributes to the overall free radical action.^{16,18} The role of the guaiacyl

moiety (i.e., *o*-OH, OCH₃ group) (Figure 1) has only been theoretically discussed in a few studies.¹⁹ However, this group is present in numerous active and well-known compounds including silybin.²² These compounds are biologically active, and those activities are often correlated with their capacity to scavenge free radicals. Thus even if the guaiacyl moiety does not confer to polyphenols the best free radical scavenging capacity as H donors, this group seems to significantly participate in the biological activities of some polyphenols.

The present paper is a joint experimental and theoretical study dealing with the role of this moiety. This study was based on a series of nine compounds all containing the guaiacyl moiety since they are dimers, trimers, and tetramers of guaiacol (2-methoxyphenol) (Figure 1). Guaiacol is isolated from the gaiac resin.²³ It is the main constituent of creosote obtained from wood tar (mainly beech).²⁴ Guaiacol and other derivatives are used as external antiseptics, gastric sedatives, flavorings, deodorants, and parasiticides. Methoxyphenols are used as antioxidants for plastics and rubbers.

In order to understand, elucidate, and predict the free radical scavenging properties of that series of compounds DFT calculations have been carried out in the gas phase and in the presence of a solvent (using a polarizable continuum model (PCM)). The capacity of H atom transfer (HAT) from each OH group was estimated by the calculation of BDEs (bond dissociation enthalpy). The capacity for electron transfer (ET) was estimated by the ionization potential (IP). The phenoxyl radicals, formed after the loss of one H atom, were also studied according to (i) their electron spin density distribution and (ii) their capacity to lose a second H atom. The results of these calculations were compared to the experimental DPPH (2,2-diphenyl-1-picrylhydrazyl)-free-radical scavenging capacity, which was measured by electron paramagnetic resonance (EPR). The thermodynamic and kinetic scheme of the free radical scavenging was theoretically established for DPPH and ROO[•] peroxy radicals (involved in lipid peroxidation). This was discussed to explain the general

* Corresponding author: P. Trouillas, Laboratoire de Biophysique EA 4021, Faculté de Pharmacie, Université de Limoges, 2 rue du Docteur Marcland, 87025 Limoges, France; tel, +33 (0) 555 435 927; fax, +33 (0) 555 435 845; e-mail, trouillas@unilim.fr.

[†] Université de Limoges.

[‡] Université Mohammed V.

[§] Service commun de RMN, Université de Limoges.

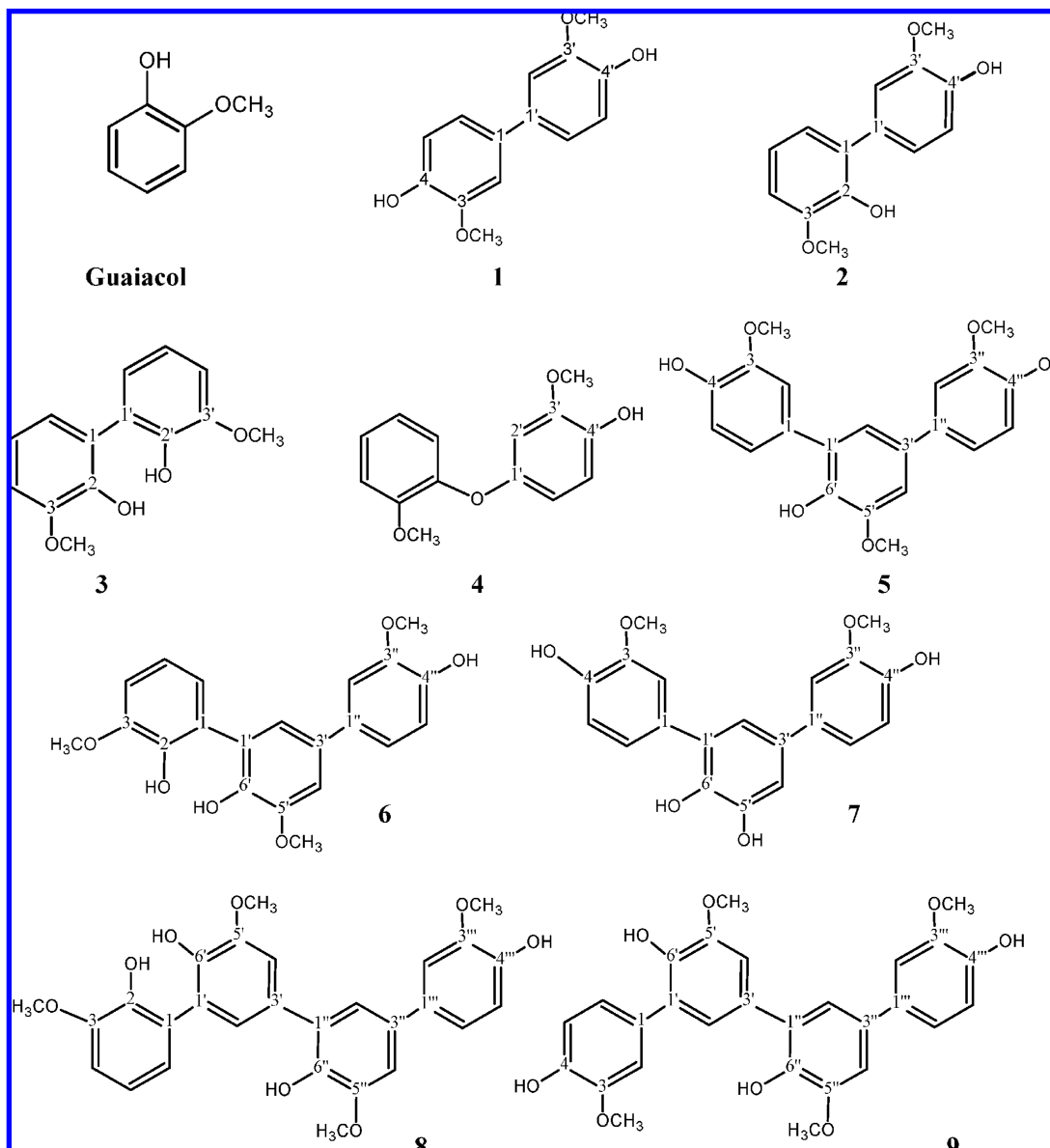


Figure 1. Chemical structures of the different synthesized guaiacol oligomers.

capacity of these compounds to scavenge ROS (reactive oxygen species) and to understand the role of the guaiacyl moiety.

Material and Methods

Enzymatic Synthesis of Compounds 1 to 9. Compounds 1 to 9 (1, 3,3'-dimethoxy-1,1'-biphenyl-4,4'-diol; 2, 3,3'-dimethoxy-1,1'-biphenyl-2,4'-diol; 3, 3,3'-dimethoxy-1,1'-biphenyl-2,2'-diol; 4, 3'-methoxy-1'-(methoxyphenoxy)phenol; 5, 3,5',3''-trimethoxy-1,1'; 3',1''-terphenyl-4,6',4''-triol; 6, 3,5',3''-trimethoxy-1,1'; 3',1''-terphenyl-2,6',4''-triol; 7, 3,3'-dimethoxy-1,1'; 3',1''-terphenyl-4,5',6',4''-tetraol; 8, 3,5',5'',3'''-tetramethoxy-1,1'; 3',1''; 3'',1'''-tetraphenyl-2,6',6'',4'''-tetraol; 9, 3,5',5'',3'''-tetramethoxy-1,1'; 3',1''; 3'',1'''-tetraphenyl-4,6',6'',4'''-tetraol) were synthesized according to a method derived from that previously described by K. E. Simmons et al.²⁶ Guaiacol (4 mM) was enzymatically oxidized by horseradish peroxidase (2 U/mL) in a citrate-phosphate buffer (pH 5.5) containing hydrogen peroxide (2 mM). The reaction was achieved at room temperature for 30 min. Enzyme activity was stopped by acidification of the reaction mixture with acetic acid. Separation was performed by MPLC, using three successive different systems:

(i) C-18 column (LiChroprep RP-18, 18–25 μ m diameter, 15 \times 230 mm) using methanol/water (60:40 to 90:10, 3 mL/min, 600 mL) as the eluant, (ii) silica gel column (Polyoprep 20–60 μ m diameter, 15 \times 230 mm) using *n*-hexane/ethyl acetate as the mobile phase (70:30 to 0:100, 3 mL/min., 500 mL), and (iii) C-18 column using methanol/water (50:50 to 90:10, 3 mL/min., 550 mL) as the eluant. Purification was achieved on a Sephadex LH-20 column (15 \times 600 mm) with methanol as the eluant.

NMR analyses are reported in the Supporting Information and confirmed the molecular structures of compounds 1 to 9 (Figure 1).

DPPH Free Radical Scavenging Capacity. Because of its paramagnetic properties, DPPH exhibits a characteristic ESR (electron spin resonance) signal. The ESR spectra were obtained with a Bruker model ESP300E spectrometer, using microsampling pipets at room temperature under the following conditions: 100 kHz modulation frequency, 9.78 GHz microwave frequency, 2mW microwave power, 1.97 modulation amplitude, and 10.24 ms time constant. The ESR spectra were recorded 3 min after sample preparation.

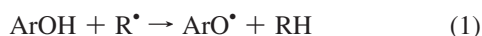
Mixtures that contained 50 μL of compound, dissolved in methanol at different concentrations, and 50 μL of DPPH ethanol solution ($5 \times 10^{-4}\text{M}$) were tested. Inhibition was calculated as follows

$$\text{inhibition} = [\text{ref} - \text{compound}] / [\text{ref} - \text{bg}]$$

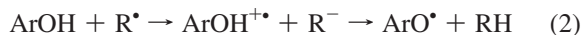
where ref and compound are the values of the double integrals for the ESR spectrum of the reference (DPPH + solvent) and the tested solution (DPPH + solvent + compound), respectively; bg represents the background signal (solvent). Each datum is the result of the average of three, independent, measurements. The IC₅₀ value was calculated from the inhibition = $f(\text{concentration})$ curves.

Theoretical Methodology. Phenolic compounds (ArOH) may scavenge free radical (R^\bullet) mainly through two different mechanisms, HAT or ET:

HAT mechanism



ET mechanism

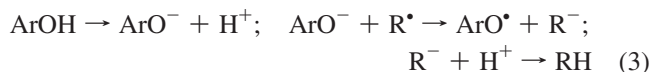


The former is a spontaneous H atom abstraction from the phenolic hydroxyl groups to the free radical. In this mechanism, the O–H bond rupture is homolytic and the capacity of this mechanism is essentially driven by the BDE physicochemical parameter. BDEs were calculated for each OH group as the difference between the $[\text{ArO}^\bullet + \text{H}^\bullet]$ and the ArOH enthalpies. The lower the BDE, the easier the O–H bond rupture and the more important its role in the antioxidant reactivity. BDE is an intrinsic parameter that helps to estimate the intrinsic capacity of the compound to lose one H atom. Nonetheless reaction 1 also depends on the R^\bullet radical reactivity and we also calculated ΔG^{HAT} (HAT-reaction-Gibbs energy). To be active on a given R^\bullet radical, the reaction must exhibit a negative ΔG^{HAT} , so that reaction 1 is thermodynamically favorable (exergonic). BDE values were calculated taking into account the zero point energy (ZPE) and the thermal contributions to translation, rotation, and vibration at 298 K.

The latter mechanism consists of two steps. The first step (electron loss or ET for electron transfer) is followed by the formation of the $\text{ArOH}^{+\bullet}$ radical cation. This mechanism is driven by IP, an intrinsic parameter, and by ΔG^{ET} Gibbs energy in the first step of reaction 2. The second step is the heterolytic O–H bond dissociation (i.e., proton loss), which is strongly exothermic. The global mechanism is so-called ET-PT. Let us note that $\Delta G^{\text{ET-PT}} = \Delta G^{\text{HAT}}$.

Actually two other mechanisms can explain the capacity of antioxidants to scavenge free radicals.

SPLET mechanism



This third mechanism is the sequential proton loss electron transfer (SPLET), in which the proton is first transferred, followed by the electron transfer.²⁷ This mechanism is favored in specific pH conditions that did not correspond to those of the DPPH scavenging measurements, as performed in the present

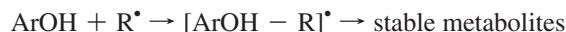
TABLE 1: O–H BDEs (kcal/mol) Obtained for Compound 1 at the B3P86 Level with the 6-31+G(d,p) and 6-311+G(2d,3pd) Basis Sets, Respectively

	4-OH		4'-OH	
	gas	solvent	gas	solvent
B3P86/6-31+G(d,p)	83.9	80.7	83.9	80.7
B3P86/6-311+G(2d,3pd)	84.1	80.7	84.1	80.7

work. In this case SPLET could participate in the global scavenging process but only as a minor mechanism. Moreover SPLET forms the same products as those obtained with the HAT and ET mechanisms and the three mechanisms are thermodynamically similar: ΔG^{SPLET} is equal to $\Delta G^{\text{ET-PT}}$ and ΔG^{HAT} and will be partly described by BDE.

The forth mechanism is adduct formation between the antioxidant and the radical:

Addition mechanism



This mechanism appears in certain conditions including reactions between (i) carbon-centered radicals and double bonds²⁸ and (ii) hydroxyl radical and aromatic rings.²⁹ As recently demonstrated and theoretically studied it is favored in radiolytic solutions.³⁰ In this case numerous side reactions may occur that help stable metabolite formation from the $[\text{ArOH} - \text{R}]^\bullet$ adduct. In the present work these metabolites were not observed and the adduct formation between DPPH and guaiacol oligomers was considered to be minor and was not studied.

All calculations presented in this work (conformational study and energy and enthalpy estimations) were carried out by using DFT methods as implemented in Gaussian03.³¹ We recently demonstrated that the B3P86 functional was particularly adapted for phenol BDEs, giving a high accuracy compared to the experimental values.¹⁶ On the basis of these studies we extrapolated the use of B3P86 to the series of phenolic compounds studied in this paper. For the dimers, two basis sets were used, 6-31+G(d,p) and 6-311+G(2d,3pd). Increasing the number of polarization function of H atoms is known to improve the O–H BDE estimation; nonetheless as can be seen in Table 1, BDEs obtained with both basis sets were very similar since they exhibited differences lower than 0.5 kcal/mol. Such a difference was low enough to be considered as a part of the global error, and for the rest of the compounds we only used the (U)B3P86/6-31+G(d,p) level of calculations. The geometries, enthalpies (H), and Gibbs energies (G) of reactants, intermediates, and products were determined by using the (U)B3P86/6-31+G(d,p) method. All the ground states were confirmed by vibrational frequency analysis, i.e., no imaginary frequency.

The transition states (TSs) were confirmed by the presence of one imaginary frequency, which was assigned to the vibration mode corresponding to the reaction studied (e.g., bond formation, bond breaking). TSs were also confirmed by IRC (intrinsic reaction coordinate) analysis. The TS Gibbs energy allowed us to evaluate the free energies of activation ΔG^\ddagger . These energies are known to be underestimated by hybrid functionals such as B3P86. More recently the MPWB1K functional appeared to be much more efficient to reproduce ΔG^\ddagger ,³² especially for H atom transfer reactions.³³ As a matter of fact all calculations concerning kinetics (i.e., reactant, product, and TS energies) were

performed for compounds **1** to **4** (dimers) at the (U)MPWB1K/6-31+G(d,p) level. Thermodynamic results (i.e., ΔH and ΔG) obtained with this method were very similar to those obtained with B3P86/6-31+G(d,p) (Supporting Information).

BDEs of each OH group were calculated for compounds **1** to **9** according to

$$\text{BDE} = H(\text{ArO}^\bullet, 298 \text{ K}) + H(\text{H}^\bullet, 298 \text{ K}) - H(\text{ArOH}, 298 \text{ K})$$

where H was the enthalpy that took into account temperature-dependent corrections (zero point energy (ZPE), translational, rotational, and vibrational energies at 298 K). $H(\text{ArOH}, 298 \text{ K})$ corresponded to the enthalpy of the molecule and $H(\text{ArO}^\bullet, 298 \text{ K})$ was the enthalpy of the phenoxy radical from where the H atom was removed. BDE of the i OH group of a compound was quoted BDE(i -OH).

BDE_D corresponded to a second H abstraction from the ArO[•] radical

$$\text{BDE}_D = H([\text{ArO}^\bullet\text{--H}], 298 \text{ K}) + H(\text{H}^\bullet, 298 \text{ K}) - H(\text{ArO}^\bullet, 298 \text{ K})$$

BDE_D(i,j) was the BDE of the j -OH group obtained from the ArO[•] radical that was formed after the H-loss from i -OH.

The solvent effects were taken into account implicitly by using a PCM (polarizable continuum model) method, since using a box of explicit solvent molecules was unfeasible with such compounds. The effects of explicit water molecules in the surrounding of the OH phenol group have been investigated,³⁴ and the authors have confirmed that the use of PCM gives a relatively good description of BDEs. We also tested hybrid models (i.e., one or two molecules in the surrounding of the OH groups + PCM) for quercetin,¹⁷ a larger system than phenol. We did observe only a slight difference in BDE as compared to a pure PCM calculation, while computational time was dramatically increased. Thus in the present paper calculations were performed with IEFPCM (integral equation formalism PCM) and UA0 radii, well-adapted for phenol BDE description (data not shown). The antioxidant test (DPPH scavenging) was performed in very polar solutions. Thus PCM calculations were performed in water ($\epsilon = 78.35$) to maximize the polarization effect as compared to vacuum calculations. Since in biological conditions antioxidants may also act in lipid membranes, the influence of the dielectric constant was also estimated using the benzene dielectric constant ($\epsilon = 2.27$). This is assumed to give a reliable approximation of the polarizable conditions of a nonpolar medium such as lipid membrane. Calculations in benzene were performed only for dimers. As can be seen in the Supporting Information, BDEs were very similar to those obtained in the gas phase, which made gas-phase calculations a reliable and easier estimation of the behavior in a nonpolar medium.

The rate constants appeared more relevant than ΔG^\ddagger to compare the different reactions since HAT reactions may involve tunneling. Rate coefficients were calculated at 298 K within the conventional TST (transition state theory) framework

$$k(T) = \kappa(T)k^{\text{TST}}(T) = \kappa(T)\frac{k_B T}{h}e^{-\Delta G^\ddagger/RT}$$

The $\kappa(T)$ transmission coefficient (quantum tunneling along the reaction coordinate) was evaluated by three different methods (Wigner, Skodje and Truhlar, and Eckart).

The Wigner method³⁵ is the most widely used and the simplest approximation to account for tunneling through the reaction barrier. This method assumes a parabolic potential for nuclear motion near the transition state and $\kappa^W(T)$ is given by

$$\kappa^W(T) = 1 + \frac{1}{24}\left[\frac{h \text{Im}(\nu^\ddagger)}{k_B T}\right]^2$$

where ν^\ddagger is the TS imaginary frequency.

It must be stressed that this approximation is valid for $k_B T \gg h \text{Im}(\nu^\ddagger)$. In our case (ν^\ddagger ranging from 500 to 1800 cm⁻¹), $h \text{Im}(\nu^\ddagger)$ is higher than $k_B T$ by about 1 order of magnitude (at 298 K).

In contrast to the Wigner method, the method of Skodje and Truhlar³⁶ depends not only on the imaginary frequency but also on the height of the potential energy barrier. The transmission coefficients are given with good accuracy^{36–38} by the following analytic expressions.

$\beta < \alpha$:

$$\kappa^{\text{ST}}(T) = \frac{\beta\pi/\alpha}{\sin(\beta\pi/\alpha)} - \frac{\beta}{\alpha - \beta}e^{[(\beta-\alpha)(\Delta V^\ddagger - V)]}$$

$\alpha < \beta$:

$$\kappa^{\text{ST}}(T) = \frac{\beta}{\beta - \alpha}(e^{[(\beta-\alpha)(\Delta V^\ddagger - V)]} - 1)$$

where $\alpha = 2\pi/(h \text{Im}(\nu^\ddagger))$, $\beta = 1/k_B T$, ΔV^\ddagger is the zero-point-including potential energy difference between TS and the reactants, and V is 0 for an exoergic reaction and the (positive) zero-point-including potential energy difference between reactants and products for an endoergic reaction.

The Eckart method,³⁹ is based on the Eckart potential which is a potential energy curve fitting based on the zero-point-energy of the reactants, the transition state, and the products. The corresponding analytical expression is given by

$$V(s) = \frac{ae^{\alpha(s-s_0)}}{1 + e^{\alpha(s-s_0)}} + \frac{be^{\alpha(s-s_0)}}{(1 + e^{\alpha(s-s_0)})^2} + c$$

where s is the reaction coordinate ($s = -\infty$, 0, and $+\infty$ for reactants, TS, and products, respectively) and a , b , c , α , and s_0 are parameters that depend on the imaginary frequency and the potential energies of reactants, TS, and products (as an example see ref 38 for analytical expressions).

Results and Discussion

Enzymatic Synthesis. Dimers, trimers, and other oligomers of polyphenols are known to be formed in plants and they are so-called procyanidins or condensed tannins in the case of flavonoids. Numerous oligomers of catechin exist, and they are classified in different subgroups depending on the carbon atoms involved in the covalent C–C bond formation.⁴⁰ The presence of other types of dimers including quercetin and phenolic acid dimers is reported as well.^{41–43}

The dimerization of polyphenols can be explained by their capacity to be oxidized. This oxidation may be initiated/

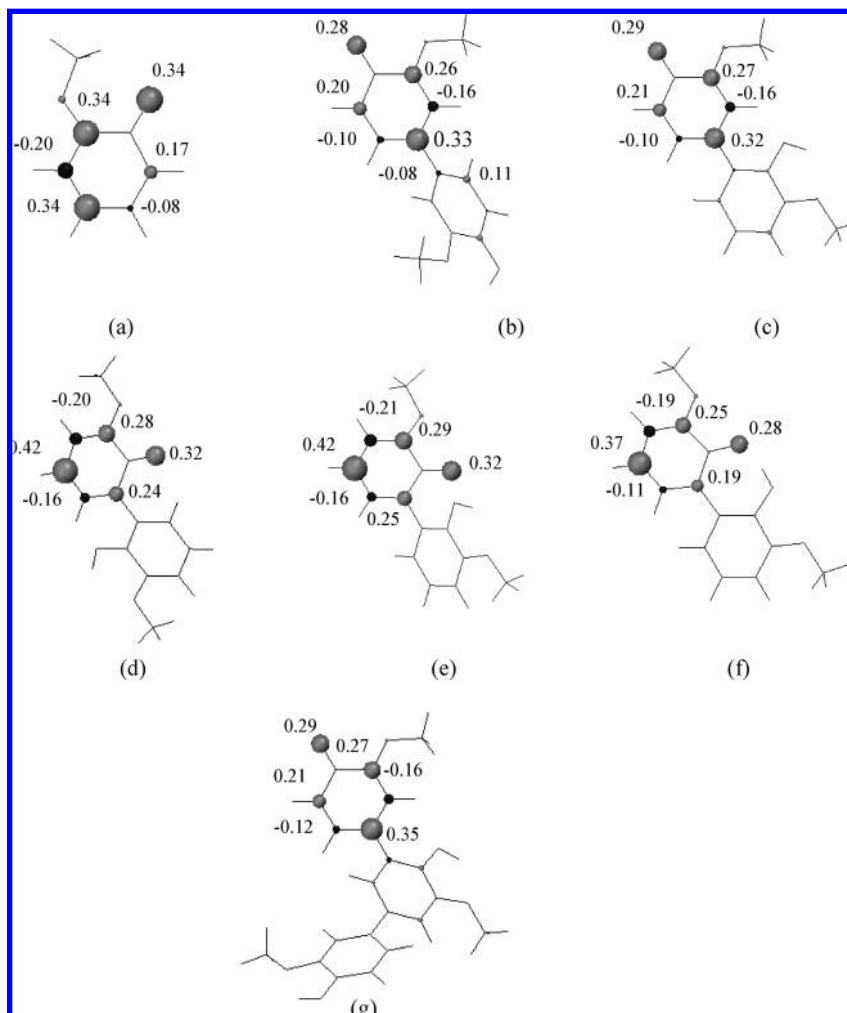


Figure 2. Spin density distribution of the ArO• phenoxy radicals obtained after one HAT from (a) the OH group of guaiacol, (b) the 4'-OH group of **1**, (c) the 4'-OH group of **2**, (d) the 2'-OH group of **3a**, (e) the 2'-OH group of **3b**, (f) the 2'-OH group of **3c**, and (g) the 4-OH group of **5**.

catalyzed chemically or enzymatically. The guaiacyl as well as the catechol moieties are known to bind to the active site of oxidative enzymes (e.g., laccases, peroxidase). The radical cation formed is very unstable, and the oxidative process is either combined or followed by a proton loss (ET-PT process), thus forming an ArO• phenoxy radical. As we calculated and as can be seen in Figure 2, the spin density distribution of this radical exhibited a strong spin density on carbon atoms C1, C3, and C5 and the oxygen atom of the phenol group. This allowed the different possibilities for C–C and C–O bond formation.

Using DFT, we theoretically studied the thermodynamics and kinetics of the C–C and C–O bond formations. As can be seen in Figure 3, the sheer bond formation (i.e., bond formation between both phenoxy radicals to form a keto-form dimer) was not very favorable with ΔG of about +1 kcal/mol. Moreover the process was relatively slow (activation barrier ΔG^\ddagger around 20 kcal/mol). It must be noticed that $\Delta H^{\text{bond-formation}}$ was negative while $\Delta G^{\text{bond-formation}}$ was positive (Figure 3 and Supporting Information). This large difference between ΔH and ΔG was attributed to the change in hybridization from $sp^2 \rightarrow sp^3$ of the carbon atom involved in the bond. This was consequently followed by a loss in planarity, thus inducing a major reorganization and thus a strong influence of entropic effects. This was confirmed by the high ΔG^\ddagger values. Nonetheless this process may quickly be followed by tautomerization to form an enol-form dimer (Figure 3), which is planar and so much more stable.

The global reaction was thus spontaneous, exhibiting a total ΔG of –45 kcal/mol.

The C–C bond formation was slightly favored as compared to the C–O bond formation, and this small difference in ΔG was enough to favor the C–C dimers since those dimers were the major compounds we obtained. Indeed in our case we did not try and guide any stereospecific dimerization, i.e., after the oxidative process, the phenoxy radicals were allowed to form bonds randomly, and we experimentally obtained much more C–C dimers than C–O dimers. Concerning the C–C dimers, C3 cannot be used for such dimerization since the presence of the methoxy group prevents tautomerization. The other three possibilities (i.e., C1–C1', C1–C5', and C5–C5') were a priori equally allowed (see Figure 3 for the theoretical prediction), and actually this is in very good agreement with our experimental evidence (e.g., similar rates for dimers **1**, **2**, and **3**). Trimer and tetramer formation followed the same logic (i.e., guaiacol or guaiacol-dimer oxidation, formation of phenoxy radicals, random bond-formation favoring C–C linkage, and tautomerization to form the final products).

Conformation Feature. It is known from the literature that flavonoid oligomers often exist as rotamers in solution.^{44,45} Here we carefully studied the potential energy surfaces of the different compounds and we indeed obtained different conformers very close in energy. In the case of dimers **1** and **2**, the potential energy surface, in which the reaction coordinate was torsion

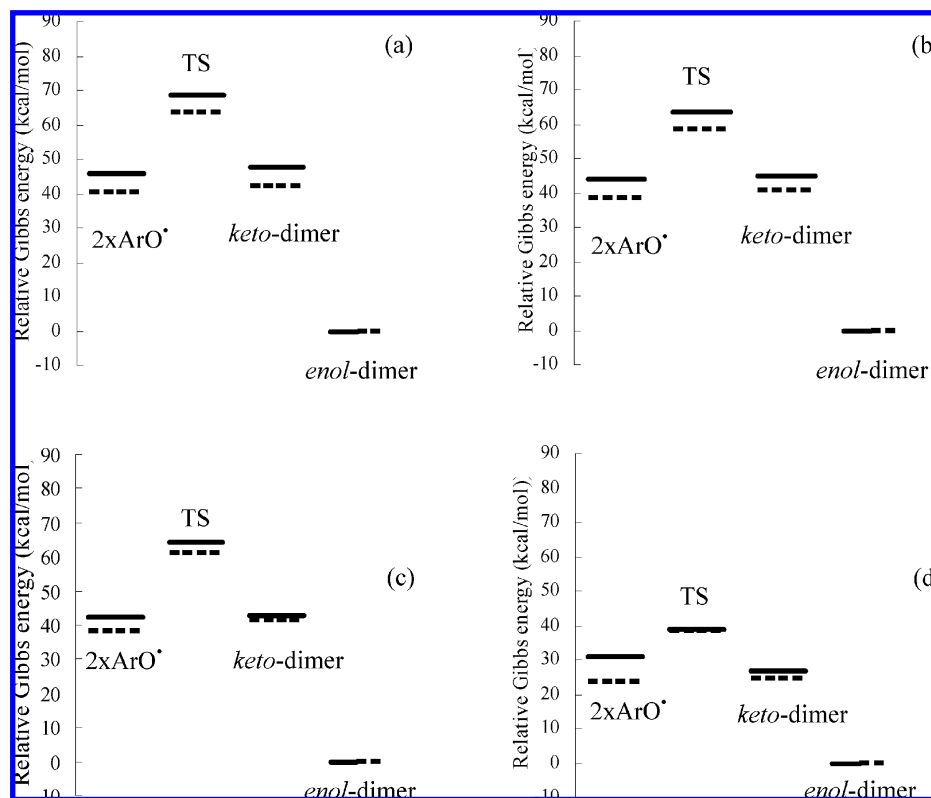


Figure 3. Thermodynamic and kinetic schemes for the (a) C1–C1', (b) C1–C5', (c) C5–C5', and (d) C–O bond formation. ΔG (kcal/mol) values are reported on the vertical axis. ArO^\bullet is the phenoxy radical obtained after guaiacol oxidation, keto- and enol-dimers are both dimer forms, and TS corresponds to the transition state of the bond formation.

TABLE 2: BDEs (kcal/mol) and IPs of the Two Conformers (1a and 1b) of Compound 1, Obtained at the B3P86/6-31+G(d,p) Level

	4-OH		4'-OH		IP	
	gas	solvent	gas	solvent	gas	solvent
1a	83.9	80.7	83.9	80.7	7.3	5.8
1b	84.0	79.6	84.0	79.5	7.3	5.8

angle τ between the aromatic rings, exhibited two potential wells at $\tau = 40^\circ$ and 140° , respectively. These two conformers were symmetric and, as we will see later, exhibited the same redox behavior (see BDEs of both conformers in Table 2). These conformers were not totally planar but however allowed conjugation over the entire molecule. As can be seen in Figure 4 for **1**, HOMO (highest occupied molecular orbital) was delocalized over the entire molecule.

In the case of dimer **3**, the first conformer (i.e., $\tau = 140^\circ$, conformer **3a**) was the same as for **1** and **2** and corresponded to the arrangement in which both OH groups were opposite to each other. Besides, the second conformer was different and the torsion angle was higher than those for **1** and **2** (i.e., $\tau = 60^\circ$ conformer **3b** compared to 40° for **1** and **2**). Such a higher torsion was attributed to the steric hindrance between oxygen atoms. Nonetheless in this case a third conformer (**3c**) exists, in which an inter-ring H-bond was formed between both OH groups. Enthalpies of the three conformers were very similar (difference lower than 0.2 kcal/mol). As can be seen in Figure 4 the conjugation between both aromatic rings is still present for **3b**.

The conformational features of trimers and tetramers were deduced from the knowledge gained on dimers. This was just a combination of the different possibilities, allowing four and eight conformers for trimers and tetramers, respectively. In the

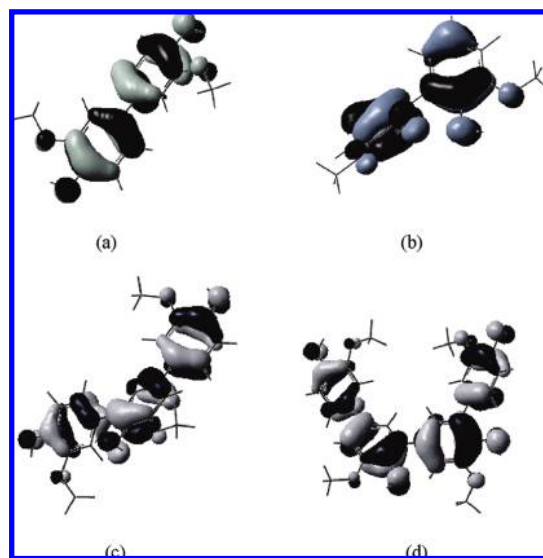


Figure 4. HOMO distribution for compounds (a) **1**, (b) **3b**, (c) **5**, and (d) **9**.

present study we only focused on one conformer as the redox properties were similar, except for **6** and **8**. In these two compounds an inter-ring H-bond was allowed (as for **3**), thus changing the redox capacity (see below). So in this case we also studied the influence of this H bonding interaction on the redox capacity and on the correlation with the free radical scavenging activity. As can be seen in Figure 4, HOMO is delocalized over the entire molecule for trimers as well as tetramers.

Concerning dimer **4**, two torsion angles τ_1 and τ_2 were investigated and the potential energy surface highlighted two

TABLE 3: BDEs Quoted BDE(*i*-OH) for the BDE of the *i*OH Group and Reported in the Gray Rows and BDE_D^a (Double BDEs) Obtained after a Second H Atom Abstraction in the White Rows: (a) In the Gas Phase and (b) in the Presence of a PCM Solvent ($\epsilon \approx 78.35$)

(a)											(b)													
	Dimers						Trimers				Tetramers		Dimers						Trimers				Tetramers	
	1	2	3a	3b	3c	4	5	6	7	8	9	1	2	3a	3b	3c	4	5	6	7	8	9		
BDE(2-OH)		83.6	84.6	85.8	81.7			84.9		83.2									82.8		82.7			
BDE _D (2,2')			-	89.0	-											87.3								
BDE _D (2,4')		80.0													78.4									
BDED(2,6')								81.0											82.5					
BDE _D (2,4'')								99.9											94.7					
BDE(4-OH)	83.9						84.7		84.9		84.0							82.0		81.7		82.1		
BDE _D (4,4')	77.2														76.2									
BDED(4,5')									68.6											76.6				
BDE _D (4,6')							77.3		78.0									78.0		78.5				
BDE _D (4,4'')							100.5		102.0									93.4		93.7				
BDE _D (2'-OH)			84.6	85.8	82.7											82.6	83.0	82.5						
BDE _D (2',2)			-	89.0	-											87.3								
BDE(4'-OH)	83.9	84.7		-	-	82.4											79.5							
BDE _D (4',2)		78.8														78.7								
BDE _D (4',4)	77.2																							
BDE(5'-OH)									76.7															
BDE _D (5',4)									77.4												81.0			
BDE _D (5',6')									74.7												76.8			
BDE _D (5',4'')									74.0												72.4			
BDE(6'-OH)							81.2	82.3	72.0	82.9	83.0							79.5	80.0	76.6	81.0	80.5		
BDE _D (6',2)								83.6											85.2					
BDE _D (6',4)							80.8		82.1									80.4		78.9				
BDE _D (6',5')									79.3											74.0				
BDE _D (6',4'')							77.4	76.1	78.7									76.3	75.6	74.5				
BDE(4''-OH)							84.1	83.6	84.4									80.9	80.6	80.7				
BDE _D (4'',2)								101.3											98.6					
BDE _D (4'',4)							101.2		102.5									94.5		94.7				
BDE _D (4'',5')							-		66.3											86.5				
BDE _D (4'',6')							74.5	74.8	66.3									75.0	75.0	73.2				
BDE(6''-OH)												81.0	81.3								79.6	80.1		
BDE(4'''-OH)												83.8	84.2								80.8	80.9		

BDE(2-OH)		81.9	82.6	82.9	81.7			82.8		82.7	
BDE _D (2,2')				87.3							
BDE _D (2,4')		78.4									
BDE _D (2,6')								82.5			
BDE _D (2,4'')								94.7			
BDE(4-OH)	80.7						82.0		81.7		82.1
BDE _D (4,4')	76.2										
BDE _D (4,5')									76.6		
BDE _D (4,6')							78.0		78.5		
BDE _D (4,4'')							93.4		93.7		
BDE _D (2'-OH)		82.6	83.0	82.5							
BDE _D (2',2)			87.3								
BDE(4'-OH)	80.7	81.6			79.5						
BDE _D (4',2)		78.7									
BDE _D (4',4)	76.2										
BDE(5'-OH)										81.0	
BDE _D (5',4)										76.8	
BDE _D (5',6')										72.4	
BDE _D (5',4'')										86.1	
BDE(6'-OH)						79.5	80.0	76.6	81.0	80.5	
BDE _D (6',2)							85.2				
BDE _D (6',4)						80.4		78.9			
BDE _D (6',5')								74.0			
BDE _D (6',4'')							76.3	75.6	74.5		
BDE(4''-OH)						80.9	80.6	80.7			
BDE _D (4'',2)							98.6				
BDE _D (4'',4)							94.5		94.7		
BDE _D (4'',5')									86.5		
BDE _D (4'',6')							75.0	75.0	73.2		
BDE(6''-OH)										79.6	80.1
BDE(4'''-OH)										80.8	80.9

^a BDE_D(*i,j*) is the BDE of the *j*-OH group obtained from the ArO radical formed after the H-loss from *i*-OH.

symmetrical different rotamers ($\tau_1 = -165^\circ$, $\tau_2 = 72^\circ$ and $\tau_1 = 162^\circ$, $\tau_2 = -72^\circ$). Their redox properties were identical, i.e., same BDEs, IPs, and HOMO distribution (data not shown).

BDE Analysis. This series of compounds allowed us to study the chemical behavior of the guaiacyl OH groups and the chemical environment's influence on their BDEs. The O–H BDEs were very similar to each other for the different compounds (Table 3). Most of them were ranging from 79.5 to 83.0 kcal/mol. These differences were relatively low but may be considered as significant enough when comparing the different BDEs to each other (BDEs calculated at the same level of calculation). Moreover the BDE values were ranging around the BDE threshold that we proposed to rationalize DPPH free radical scavenging.¹⁸ Thus one can imagine that the difference observed in this very range could be of importance.

The major difference between the guaiacyl O–H BDEs was observed for the OH groups involved in the inter-ring H bonding interactions, i.e., for compounds **3**, **6**, and **8**. Let us explore carefully the difference in behavior between the different conformers of **3**. For conformer **3a** the two OH groups were obviously totally symmetrical and both BDEs were the same. For conformer **3c**, the BDE of the OH group involved in the inter-ring H bonding was lower by about 1.0 kcal/mol. This was due to a better stabilization of the corresponding radical due to (i) a lower spin density delocalization (0.28 on the O-atom vs 0.32 for **3c** and **3a/3b**, respectively) (Figure 2) and (ii) a strong H-bonding stabilization (i.e., distance between the OH group and the O-atom of about 1.55 Å). Because the different conformers possess very similar energies, they probably have the same Boltzmann repartition in solution, and the actual BDE is probably an average of the different values. For compounds

3, **6**, and **8**, BDEs were higher than those of compound **1** by about 1 kcal/mol in water (Table 3).

Other slight differences are also reported in Table 3. The 4'-OH group of compound **2** exhibited a BDE higher by about 1 kcal/mol than that of compound **1**. This is due to the different chemical environment and the subsequent difference in the mesomeric effects of both compounds. The radical obtained from the former compound was more delocalized over the whole structure. This was confirmed by (i) a lower spin density on the O-atom and a better delocalization to the second aromatic ring for **1** compared to **2** (Figure 2) and (ii) a more planar structure for **1** compared to **2** ($\tau = 27^\circ$ and 35° , respectively). This effect was also observed for the 4-OH group of **5** and the 4-OH group of **9**, which indeed possess the same chemical environment difference as **1** vs **2**.

The catechol OH BDEs of **7** (i.e., 81.0 and 76.6 kcal/mol for 5'- and 6'-OH, respectively) were lower than the guaiacyl BDEs (Table 3). This was especially true for the 6'-OH group and was in agreement with the different theoretical studies reporting on the O–H BDEs of catechol moieties in quercetin,^{12,16} chalcones,¹⁷ and catechins,⁹ in which these moieties appeared to be very effective H donors.

DPPH Free Radical Scavenging Capacity. On the basis of the IC₅₀ values we obtained and that we report in Table 4, the following hierarchy was obtained for the DPPH free radical scavenging of dimers: **1** > **2** > **3** > **4**. Concerning **1**, **2**, and **3**, the BDE was relatively well correlated with this activity since the OH BDE of **1** was the lowest and the BDE of **3** was the highest. The relatively low activity of **4** did not come from a higher BDE value but more probably from the number of OH

TABLE 4: DPPH Free Radical Scavenging IC50s (concentration required to scavenge 50% of DPPH radicals) of Compounds 1 to 9

compound	IC50 (μ M)	compound	IC50 (μ M)
1	55.6	6	66.5
2	72.2	7	61.0
3	89.6	8	40.5
4	93.2	9	36.5
5	52.7		

groups (one for **4** and two for **1**, **2**, and **3**), as we will develop later in the paper.

Concerning trimers the following hierarchy was obtained: **5** > **7** > **6**. The better activity obtained for **5** compared to **6** seemed to be consistent with the results obtained for dimers, i.e., relatively well-correlated to the H donor capacity. Nonetheless the relatively low free radical scavenging of **7** was definitely not consistent with the theoretical prediction of the H donor capacity. This result was neither consistent with the good antioxidant role of the catechol moiety generally observed for polyphenols. Actually on the basis of the theoretical prediction, a thorough analysis of **7** was achieved and indicated that this compound was not stable and was transformed in the solution during the DPPH scavenging test. Subsequently the actual concentration of **7** appeared to be very poor in this solution. In conclusion the antioxidant evaluation of **7** was not possible with this test, and the comparison with other compounds was thus unfeasible.

Concerning the tetramers, **9** was more active than **8**. This was again partly attributed to the higher BDE obtained in **8** as compared to **9**. Nonetheless in this case the difference was almost nonsignificant and this only concerned one of the four groups; thus the correlation with BDE was far from perfect.

Number of OH Groups. Globally speaking (i.e., for the whole series) and ignoring compound **7**, one can observe that tetramers were more active than trimers, which were a little bit more active than dimers, which were more active than the dimer with one OH group (**4**). Thus the number of OH groups was of great importance and influenced the global free radical scavenging capacity. The present study was particularly well-adapted to highlight the importance of this parameter since each individual OH group exhibited a very similar behavior (i.e., very similar capacity as H donor).

A Second HAT Possibility. After the first HAT (or ET-PT) an ArO^\bullet radical was formed. The stability and the reactivity of these radicals have not been widely studied in the literature. At that point, because the correlation between BDEs and the observed experimental activities was not perfect, we investigated the capacity of those ArO^\bullet radicals to react with free radicals (e.g., DPPH). We investigated the capacity of a second HAT (or ET-PT) mechanism. The physicochemical parameter which was calculated was so-called $\text{BDE}_D(i,j)$ for the BDE of the j -OH group obtained from the ArO^\bullet radical formed after the H-loss from i -OH.

The results obtained for dimers and trimers (Table 3) were crucial to establish the structure–activity relationship. Indeed, BDE_D s were relatively low (ranging from 76.2 to 87.3 kcal/mol), which demonstrated the high antioxidant capacity of the ArO^\bullet radical formed, in solution, after a first HAT action. This high capacity comes from the fact that the product formed after the second HAT was stabilized in a sheer singlet state (spin multiplicity of 1) and not in a triplet state (spin multiplicity of 3). The former was more stable than the latter by about 13 kcal/mol. Such a stabilization in a singlet state favored the capacity of two rather than only one HAT in solution.

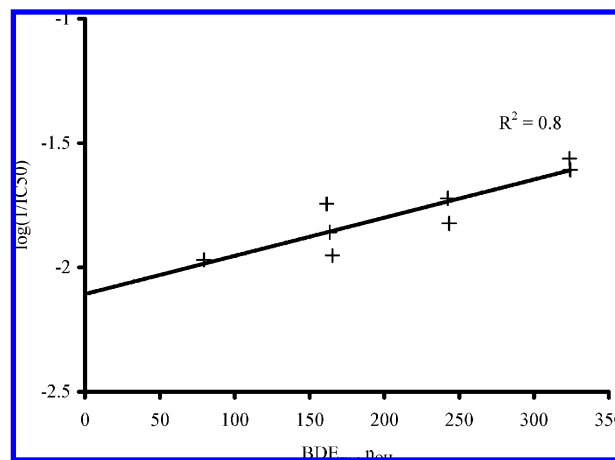


Figure 5. $\log(1/\text{IC}_{50})$ vs $\text{BDE}_{\text{av}} \times n_{\text{OH}}$ (for the different compounds) and the corresponding linear regression. For each compound the $\log(1/\text{IC}_{50})$ value represents the DPPH free radical scavenging activity, BDE_{av} is the average of the O–H BDEs, and n_{OH} is the number of OH group(s).

The reliability of this result was reinforced by the better correlation with the experimental free radical scavenging capacity. Indeed the BDE_D was relatively low for the different OH groups except for the OH groups involved in the inter-ring H bond. In such a case (i.e., compounds **3**, **6**, and **8**) a strong H bonding stabilized the ArO^\bullet radical making the O–H bond rupture an unfavorable event, since in addition to the sheer covalent O–H bond rupture the H bond rupture additionally cost ~ 2.5 kcal/mol. This much more significant difference in enthalpy (compared to the first HAT) explained the better antioxidant capacity of **1** and **2** compared to **3** and, even better, compared to **4** (for which a second HAT was obviously not possible).

The same explanation was proposed to explain the difference in the activity between **5** and **6** or **8** and **9**. The bigger the oligomer, the lower this effect, since for example for **9** the first, then the second HAT can occur on four different sites.

This work focused on a few major descriptors (i.e., BDE, BDE_D , and n_{OH}). In order to confirm the quality of the relationship between DPPH scavenging and these very descriptors, a linear regression was proposed between $\log(1/\text{IC}_{50})$ and BDE_{av} multiply by n_{OH} (Figure 5), where BDE_{av} was the average BDE value for each compound. The parameter “ BDE_{av} multiply by n_{OH} ” took into account BDE, BDE_D , and n_{OH} . As can be seen in Figure 5, the regression coefficient was around 0.8, making BDE, BDE_D , and n_{OH} three major descriptors to describe the free radical scavenging activity. Such a regression coefficient proved the quality of the relationship obtained between the activity and these three parameters. This was especially true because usually getting a reliable QSAR formula requires more than 30 compounds and more than three descriptors.

Thermodynamics of the $\text{ArOH} + \text{R}^\bullet \rightarrow \text{ArO}^\bullet + \text{RH}$ Reaction. In order to correlate theoretical evaluations and the experimental results reported in the present paper (i.e., DPPH scavenging activities), the Gibbs energies (ΔG) were calculated for the reaction between oligomers **1–9** and DPPH. As a comparison ΔG values are also reported (Table 5) for the reaction with peroxy radicals ROO^\bullet that are formed during the lipid peroxidation process. As a first estimation of the antioxidant capacity, the DPPH free radical scavenging has been widely used in the literature. This scavenging activity often correlates with lipid peroxidation inhibition.¹⁹ This is essentially attributed to the correlation between the sheer free radical

TABLE 5: Thermodynamics (ΔG^{HAT} and ΔG^{ET} in kcal/mol) of the DPPH and $\text{CH}_3\text{OO}^\bullet$ Free Radical Scavenging by 1–9^a

(a) First HAT								
	HAT mechanism				ET mechanism			
	ΔG^{HAT} with DPPH		ΔG^{HAT} with $\text{CH}_3\text{OO}^\bullet$		ΔG^{ET} with DPPH		ΔG^{ET} with $\text{CH}_3\text{OO}^\bullet$	
	gas	solvent	gas	solvent	gas	solvent	gas	solvent
1 (4'-OH)	4.5	5.3	0.0	-7.5	78.8	12.0	133.9	25.9
2 (4'-OH)	5.2	6.3	0.7	-6.6	81.5	15.6	136.7	29.5
3 (2-OH)	6.2	7.5	1.7	-5.4	85.6	20.3	140.7	34.2
4 (4'-OH)	3.0	4.1	-1.5	-8.8	82.1	15.2	137.2	29.0
5 (6'-OH)	1.4	4.6	-3.1	-8.2	73.2	11.8	128.3	25.7
6 (6'-OH)	2.0	5.3	-2.5	-7.5	72.5	11.9	127.6	25.7
8 (6''-OH)	1.7	0.8	-2.3	-8.4	69.0	12.0	124.5	25.5
9 (6''-OH)	2.0	1.3	-2.0	-7.8	70.5	12.1	126.0	25.6

(b) Second HAT								
	HAT mechanism				ET mechanism			
	ΔG^{HAT} with DPPH		ΔG^{HAT} with $\text{CH}_3\text{OO}^\bullet$		ΔG^{ET} with DPPH		ΔG^{ET} with $\text{CH}_3\text{OO}^\bullet$	
	gas	solvent	gas	solvent	gas	solvent	gas	solvent
1 (4',4)	-2.0	1.0	-6.5	-11.8	78.7	12.3	141.1	26.2
2 (4',2)	-0.7	4.2	-5.2	-8.6				
3 (2,2')	10.1	13.5	5.6	0.7				
5 (6',4'')	-1.9	0.8	-6.4	-12.0				
6 (6',4'')	-2.9	0.2	-7.4	-12.6				

^a Part a corresponds to the first HAT (ΔG^{HAT}) or to the electron transfer from ArOH (ΔG^{ET}). In the former case the OH number from where the H atom is removed is quoted in parentheses after the compound's name. Part b corresponds to a second HAT (ΔG^{HAT}) or electron transfer (ΔG^{ET}) from the ArO^\bullet radical obtained after the first HAT. The OH group numbers involved in both HAT are quoted in parentheses (**1**(4',4) means that we removed two H atoms from the 4 and 4'-OH groups of compound **1**).

TABLE 6: Kinetics of the $\text{CH}_3\text{OO}^\bullet$ Free Radical Scavenging by 1–5^a

(a) In the Gas Phase						
HAT reactions	ΔG^\ddagger	k^{TST}	$k^{\text{TST/W}}$	$k^{\text{TST/ST}}$	$k^{\text{TST/E}}$	
1 + $\text{CH}_3\text{OO}^\bullet \rightarrow [\text{1-H}]^\bullet + \text{CH}_3\text{OOH}$	25.1	1.3×10^{-4}	8.6×10^{-4}	0.2	0.1	
2 + $\text{CH}_3\text{OO}^\bullet \rightarrow [\text{2-H}]^\bullet + \text{CH}_3\text{OOH}$	22.1	1.1×10^{-2}	6.5×10^{-2}	5.3	1.3	
3 + $\text{CH}_3\text{OO}^\bullet \rightarrow [\text{3-H}]^\bullet + \text{CH}_3\text{OOH}$	21.9	1.4×10^{-2}	8.1×10^{-2}	2.6	2.9	
4 + $\text{CH}_3\text{OO}^\bullet \rightarrow [\text{4-H}]^\bullet + \text{CH}_3\text{OOH}$	20.9	8.0×10^{-2}	3.9×10^{-1}	2.8×10^1	4.8×10^1	
$[\text{1-H}] + \text{CH}_3\text{OO}^\bullet \rightarrow [\text{1-2H}] + \text{CH}_3\text{OOH}$	23.9	5.1×10^{-4}	3.45×10^{-3}	0.8	2.2	

(b) In the Presence of a PCM Solvent						
HAT reactions	ΔG^\ddagger	k^{TST}	$k^{\text{TST/W}}$	$k^{\text{TST/ST}}$	$k^{\text{TST/E}}$	
1 + $\text{CH}_3\text{OO}^\bullet \rightarrow [\text{1-H}]^\bullet + \text{CH}_3\text{OOH}$	22.6	3.4×10^{-1}	2.4	3.2×10^3	2.8×10^2	
2 + $\text{CH}_3\text{OO}^\bullet \rightarrow [\text{2-H}]^\bullet + \text{CH}_3\text{OOH}$	24.1	1.4×10^{-2}	0.1	4.6×10^2	2.4×10^1	
4 + $\text{CH}_3\text{OO}^\bullet \rightarrow [\text{4-H}]^\bullet + \text{CH}_3\text{OOH}$	21.6	1.0	5.7	7.9×10^2	1.9×10^2	
$[\text{1-H}] + \text{CH}_3\text{OO}^\bullet \rightarrow [\text{1-2H}] + \text{CH}_3\text{OOH}$	27.2	7.8×10^{-5}	6.2×10^{-4}	8.3×10^1	1.7	

^a The activation free energies ΔG^\ddagger are in kcal/mol and the rate coefficients are in $\text{L} \cdot \text{mol}^{-1} \cdot \text{s}^{-1}$, at 298 K. k^{TST} , $k^{\text{TST/W}}$, $k^{\text{TST/ST}}$, and $k^{\text{TST/E}}$ are the rate coefficients without tunneling corrections and taking into account Wigner, Skodje and Truhlar, and Eckart corrections, respectively. $[\text{1-H}]^\bullet$ corresponds to the phenoxy radical obtained after HAT from compound **1**. $[\text{1-2H}]$ thus corresponds to a double HAT from compound **1**. The calculations are performed with (U)MPWB1K/6-31+G(d,p) (Table 6a) in the gas phase and (Table 6b) in the presence of a PCM solvent ($\epsilon = 78.35$).

scavenging capacities of radicals involved in both tests (i.e., DPPH and ROO^\bullet , respectively).⁴⁷ For both free radicals the HAT and ET mechanisms were studied (see ΔG^{HAT} and ΔG^{ET} values, respectively, in Table 5).

As previously observed the ΔG^{ET} values were strongly influenced by the PCM solvent^{17,18} which induces a huge decrease by about 65 kcal/mol (from gas to solvent). Even in solvent, the sheer ET mechanism was endoergic. ΔG^{ET} was around 12 and 25 kcal/mol with DPPH and ROO^\bullet , respectively. It must be stressed that the ET physical process is just a step. It is followed by heterolytic bond dissociation and at the end $\Delta G^{\text{ET-PT}} = \Delta G^{\text{HAT}}$.

As can be seen in Table 5a, the first HAT from the polyphenols to the DPPH radicals was endoergic. Indeed even

if the ΔG^{HAT} values were relatively small they were significantly positive. Thus for the polyphenols studied in the present publication, the capacity to scavenge DPPH free radical by only one H atom transfer was not very effective. Besides ΔG^{HAT} values were investigated for a second HAT (i.e., H-transfer from an ArO^\bullet intermediate radical to another DPPH free radical) (Table 5b). This second reaction is thermodynamically more favorable than the first HAT, except for **3** for which the inter-ring H bonding weakened the second HAT (see text above). As a matter of fact the antioxidant action of **1** and **2** probably occurs in two steps (i.e., two HAT reactions) to establish the equilibrium. Compound **4** was much less active than **1** and **2**, since it has only one OH group. Compound **3** was less active than **1** and **2** since its capacity for a second HAT is much less

favorable. Finally **5**–**9** were more active since they probably have the capacity for a third and a fourth HAT.

As a comparison ΔG^{HAT} values were also estimated for the reaction between compounds **1**–**9** and ROO \cdot (Tables 5a and b). The previous conclusion must be modulated since all of the compounds may also be considered as good candidates for a first H donation to those types of free radicals. The second HAT was still favored except for **3**. The structure–activity relationship was theoretically the same for both radicals.

Kinetics of the ArOH + R \cdot \rightarrow ArO \cdot + RH Reaction. As thermodynamics of HAT and ET-PT are identical, the respective contributions of both mechanisms must be evaluated from the kinetic point of view. The activation barriers ΔG^\ddagger and rate constants k^{TST} were calculated for HAT from **1**–**4** to the ROO \cdot radical (Table 6). The HAT kinetics was very similar for the four compounds in the presence of a nonpolar solvent (gas phase calculations). In a polar solvent the rate was slightly slowed down for the second HAT. Globally the HAT mechanism was lowered from these compounds as compared to very active compounds such as catechin. In this compound the catechol moiety exhibited rates around $10^4 \text{ L}\cdot\text{mol}^{-1}\cdot\text{s}^{-1}$ (MPWB1K calculations in the gas phase).³³ Tunneling was relatively important and significantly changed HAT rates, according the Skodje and Truhlar and Eckart methodologies.

According to the thermodynamics data of ET-PT, the first step (i.e., ET) was clearly the limiting step (e.g., for compound **1**, $\Delta G^{\text{ET}} = +25.9 \text{ kcal/mol}$ and $\Delta G^{\text{PT}} = -33.4 \text{ kcal/mol}$ for ROO \cdot). The ET transition states have not exactly been calculated but the activation free energy was obviously higher than ΔG^{ET} (i.e., higher than 26 kcal/mol). The transition state is close to the energy required for a vertical transition, which was calculated to be at least 3–4 kcal/mol higher than ΔG^{ET} . Thus the energy of activation would be significantly higher for ET than for the first HAT (HAT from the parent molecule), which makes the sheer ET rates higher than those of HAT. This would indicate that HAT was faster than ET-PT. So HAT appeared as a major mechanism while ET-PT would be minor for this series of compounds as lipid peroxidation inhibitors. Nonetheless depending on the reactant complexes, tunneling may increase ET rates making ET-PT a competitive process compared to HAT.

The relatively small barriers (or high rate constants) obtained for the major mechanism (HAT) seemed to indicate that the reaction is mainly thermodynamically governed (i.e., not kinetically limited). This confirms the importance of the thermodynamic parameters (BDE, BDE_D, and ΔG^{HAT}) to estimate the antioxidant capacity and to establish structure–activity relationships.

More than understanding the antioxidant reactivity of that series of guaiacol oligomers, the present publication helps to understand the redox behavior of the guaiacyl moiety widely present in active polyphenols. On the basis of different arrangements of two, three, or four guaiacyl moieties, we established the (i) structure–activity relationship (see discussion and Figure 5), (ii) the role of the guaiacyl group, and (iii) the influence of its chemical environment. The crucial role of a second HAT to form a closed shell structure has also been highlighted. As far as the chemical environment allowed such a process, the BDE_D parameter (related to this capacity) must definitely be viewed as a parameter that cannot be ignored in QSAR (quantitative structure activity relationship) studies of polyphenols. The comparison of these parameters for a series of compounds must be based on accurate calculations since we concluded that small differences may influence the biological activities. It must be stressed that the solvent influence was relatively weak, essentially on the thermodynamical data. This indicated that the

difference in reactivity between compounds **1**–**9** (i.e., the structure–activity relationship) will be very similar in polar solution and in nonpolar medium such as lipid membranes.

Acknowledgment. The authors thank the “Conseil Régional du Limousin” for financial support and CALI (CALcul en Limousin) and IDRIS (Institut du Développement et des Ressources Informatiques Scientifiques, Orsay, Paris) for computing facilities. The authors are grateful to Sylvie Gautier for fruitful discussions that have helped to improve the quality of this paper.

Supporting Information Available: Cartesian coordinates xyz of compounds **1**–**9**, NMR analyses, enthalpies and free energies of the dimerization process, BDEs obtained for dimers at the MPWB1K/6-31+G(d,p) level in the gas phase and in the presence of a PCM solvent (with the water dielectric constant), and BDEs obtained for dimers at the B3P86/6-31+G(d,p) level in the presence of a PCM solvent (with the benzene dielectric constant). This material is available free of charge via the Internet at <http://pubs.acs.org>.

References and Notes

- (1) Cadenas, E.; Packer, L. *Handbook of antioxidants*, 2nd ed.; Marcel Dekker: New York, 2002.
- (2) Rice-Evans, C. A.; Miller, N. J.; Paganga, G. *Free Radical Biol. Med.* **1996**, *20*, 933.
- (3) Pietta, P. G. *J. Nat. Prod.* **2000**, *63*, 1035.
- (4) Simonetti, P.; Gardana, C.; Pietta, P. G. *J. Agric. Food Chem.* **2001**, *49*, 5964.
- (5) Charrouf, Z.; Hilali, M.; Jauregui, O.; Soufiaoui, M.; Guillaum, D. *Food Chem.* **2007**, *100*, 1398.
- (6) Van Acker, S. A. B. E.; De Groot, M. J.; Van den Berg, D. J.; Tromp, M. N. J. L.; Den Kelder, G. D. O.; Van der Vijgh, W. J. F. *Chem. Res. Toxicol.* **1996**, *9*, 1305.
- (7) Lemańska, K.; Szymusiak, H.; Tyrakowska, B.; Zieliński, R.; Soffers, A. E. M. F.; Rietjens, I. M.; C, M. *Free Radical Biol. Med.* **2001**, *31*, 869.
- (8) Priyadarsini, K. I.; Maity, D. K.; Naik, G. H.; Kumar, M. S.; Unnikrishnan, M. K.; Satav, J. G.; Mohan, H. *Free Radical Biol. Med.* **2003**, *35*, 475.
- (9) Zhang, H. Y.; Wang, L. F. *J. Phys. Chem. A* **2003**, *107*, 11258.
- (10) Martins, H. F. P.; Paulo Leal, J.; Tereza Fernandez, M.; Lopes, V. H. C.; Nata'lia Cordeiro, M. D. S. *J. Am. Soc. Mass Spectrom.* **2004**, *15*, 848.
- (11) Leopoldini, M.; Pitarch, I. P.; Russo, N.; Toscano, M. *J. Phys. Chem. A* **2004**, *108*, 92.
- (12) Leopoldini, M.; Marino, T.; Russo, N.; Toscano, M. *Theor. Chem. Acc.* **2004**, *111*, 210.
- (13) Fiorucci, S.; Golebiowski, J.; Cabrol-Bass, D.; Antonczak, S. *ChemPhysChem.* **2004**, *5*, 1726.
- (14) Lameira, J.; Medeiros, I. G.; Reis, M.; Santos, A. S.; Alves, C. N. *Bioorg. Med. Chem.* **2006**, *14*, 7105.
- (15) Zhang, H. Y.; Ji, H. F. *New J. Chem.* **2006**, *30*, 503.
- (16) Trouillas, P.; Marsal, P.; Siri, D.; Lazzaroni, R.; Duroux, J. L. *Food Chem.* **2006**, *97*, 679.
- (17) Kozłowski, D.; Trouillas, P.; Calliste, C.; Marsal, P.; Lazzaroni, R.; Duroux, J. L. *J. Phys. Chem. A* **2007**, *111*, 1138.
- (18) Kozłowski, D.; Marsal, P.; Steel, M.; Mokri, R.; Duroux, J. L.; Lazzaroni, R.; Trouillas, P. *Radiat. Res.* **2007**, *168*, 243.
- (19) Trouillas, P.; Marsal, P.; Svobodová, A.; Vostálová, J.; Gažák, R.; Hrbáč, J.; Sedmera, P.; Křen, V.; Lazzaroni, R.; Duroux, J. L.; Walterová, D. *J. Phys. Chem. A* **2008**, *112*, 1054.
- (20) Leopoldini, M.; Russo, N.; Toscano, M. *J. Agric. Food Chem.* **2007**, *55*, 7944.
- (21) Leopoldini, M.; Russo, N.; Toscano, M. *J. Agric. Food Chem.* **2006**, *54*, 3078.
- (22) Leopoldini, M.; Marino, T.; Russo, N.; Toscano, M. *J. Phys. Chem. A* **2004**, *108*, 4916.
- (23) Leopoldini, M.; Russo, N.; Chiodo, S.; Toscano, M. *J. Agric. Food Chem.* **2006**, *54*, 6343.
- (24) Gažák, R.; Svobodová, A.; Prsotová, J.; Sedmera, P.; Přikrylová, V.; Walterová, D.; Křen, V. *Bioorg. Med. Chem.* **2004**, *12*, 5677.
- (25) Sobreto, Ann. **1843**, *48*, 19.
- (26) McGinness, J. D.; Whittenbaugh, J. A.; Lucchesi, C. A. *Tappi* **1960**, *43*, 1027.
- (27) Markey, C. M.; Alward, A.; Weller, P. E.; Marnett, L. J. *J. Biol. Chem.* **1987**, *262*, 6266.

- (26) Simmons, K. E.; Minard, R. D.; Bollag, J. M. *J. Soil. Sci. Soc. Am.* **1988**, *52*, 1356.
- (27) Litwinienko, G.; Ingold, K. U. *J. Org. Chem.* **2004**, *69*, 5888.
- (28) Mokri, R.; Trouillas, P.; Kaoudji, M.; Champavie, Y.; Houée-Lévin, C.; Calliste, C. A.; Duroux, J. L. *Radiat. Res.* **2006**, *165*, 730.
- (29) Solar, S.; Solar, W.; Getoff, N. *J. Phys. Chem.* **1984**, *88*, 2091.
- (30) Anouar, E.; Košinová, P.; Kozłowski, D.; Mokri, R.; Duroux, J. L.; Trouillas, P. *Phys. Chem. Chem. Phys.* **2009**, *11*, 7659.
- (31) Frisch, M. J.; Trucks, G. W.; Schlegel, H. B.; Scuseria, G. E.; Robb, M. A.; Cheeseman, J. R.; Montgomery, J. A., Jr.; Vreven, T.; Kudin, K. N.; Burant, J. C.; Millam, J. M.; Iyengar, S. S.; Tomasi, J.; Barone, V.; Mennucci, B.; Cossi, M.; Scalmani, G.; Rega, N.; Petersson, G. A.; Nakatsuji, H.; Hada, M.; Ehara, M.; Toyota, K.; Fukuda, R.; Hasegawa, J.; Ishida, M.; Nakajima, T.; Honda, Y.; Kitao, O.; Nakai, H.; Klene, M.; Li, X.; Knox, J. E.; Hratchian, H. P.; Cross, J. B.; Bakken, V.; Adamo, C.; Jaramillo, J.; Gomperts, R.; Stratmann, R. E.; Yazyev, O.; Austin, A. J.; Cammi, R.; Pomelli, C.; Ochterski, J. W.; Ayala, P. Y.; Morokuma, K.; Voth, G. A.; Salvador, P.; Dannenberg, J. J.; Zakrzewski, V. G.; Dapprich, S.; Daniels, A. D.; Strain, M. C.; Farkas, O.; Malick, D. K.; Rabuck, A. D.; Raghavachari, K.; Foresman, J. B.; Ortiz, J. V.; Cui, Q.; Baboul, A. G.; Clifford, S.; Cioslowski, J.; Stefanov, B. B.; Liu, G.; Liashenko, A.; Piskorz, P.; Komaromi, I.; Martin, R. L.; Fox, D. J.; Keith, T.; Al-Laham, M. A.; Peng, C. Y.; Nanayakkara, A.; Challacombe, M.; Gill, P. M. W.; Johnson, B.; Chen, W.; Wong, M. W.; Gonzalez, C.; Pople, J. A. *Gaussian 03, Revision C.02*; Gaussian, Inc.: Wallingford, CT, 2004.
- (32) Zhao, Y.; Truhlar, D. G. *J. Phys. Chem. A* **2004**, *108*, 6909.
- (33) Tejero, I.; Gonzalez-Garcia, N.; Gonzalez-Lafont, A.; Lluch, J. M. *J. Am. Chem. Soc.* **2007**, *129*, 5846.
- (34) Guerra, M.; Amorati, R.; Pedulli, G. F. *J. Org. Chem.* **2004**, *69*, 5460.
- (35) Wigner, E. *J. Chem. Phys.* **1937**, *5*, 720.
- (36) Skodje, R. T.; Truhlar, D. G.; Garrett, B. C. *J. Phys. Chem.* **1981**, *85*, 3019.
- (37) Cramer, C. J. *Essentials of computational chemistry; Theories and Models*, 2nd ed.; Wiley: New York, 2004.
- (38) Vandeputte, A. G.; Sabbe, M. K.; Reyniers, M. F.; Van Speybroeck, V.; Waroquier, M.; Marin, G. B. *J. Phys. Chem. A* **2007**, *111*, 11771.
- (39) Eckart, C. *Phys. Rev.* **1930**, *35*, 1303. Zhang, Shaowen; Truong, Thanh N. *VKLab version 1.0*; University of Utah, 2001.
- (40) Harborne, J. B.; Mabry, T. J.; Mabry, H. *The Flavonoids*; Chapman and Hall: London, 1975.
- (41) Ly, T. N.; Hazama, C.; Shimoyamada, M.; Ando, H.; Kato, K.; Yamauchi, R. *J. Agric. Food Chem.* **2005**, *53*, 8183.
- (42) Ralph, J.; Quideau, S.; Grabber, J. H.; Hatfield, R. D. *J. Chem. Soc.* **1994**, *23*, 3485.
- (43) Sang, S.; Cheng, X.; Stark, R. E.; Rosen, R. T.; Yang, C. S.; Ho, C. T. *Bioorg. Med. Chem.* **2002**, *10*, 2233.
- (44) Salas, E.; Le Guernevé, C.; Fulcrand, H.; Poncet-Legrand, C.; Cheynier, V. *Tetrahedron Lett.* **2004**, *45*, 8725.
- (45) Fossen, T.; Rayyan, S.; Andersen, Ø. M. *Phytochemistry* **2004**, *65*, 1421.
- (46) $\text{CH}_3\text{OO}^\bullet$ is taken as a reliable prototype to describe the ROO^\bullet radical properties.
- (47) The compound lipophilicity may influence the structure–activity relationship obtained with both antioxidant tests (DPPH scavenging and lipid peroxidation inhibition), since this parameter strongly modulates the lipid peroxidation inhibition. See for example ref 19 and Calliste, C. A.; Kozłowski, D.; Duroux, J. L.; Champavie, Y.; Chulia, A. J.; Trouillas, P. *Food Chem.* doi: 10.1016/j.foodchem.2009.05.010.

JP906285B